

## Mapping Projected Potential, Interfacial Roughness, and Composition in General Crystalline Solids by Quantitative Transmission Electron Microscopy

P. Schwander, C. Kisielowski, M. Seibt, F. H. Baumann, Y. Kim, and A. Ourmazd

*AT&T Bell Laboratories, Holmdel, New Jersey 07733*

(Received 17 August 1993)

We describe how general lattice images may be used to measure the variation of the potential in crystalline solids in any projection, with no knowledge of the imaging conditions. This approach is applicable to structurally perfect samples, in which interfacial topography or changes in composition are of interest. We present the first atomic-level topographic map of a Si/SiO<sub>2</sub> interface in plan view, and the first microscopic compositional map of a Si/GeSi/Si quantum well in cross section.

PACS numbers: 61.16.Bg, 68.35.-p

Lattice images, obtained by transmission electron microscopy (TEM), are routinely used to infer the subsurface microstructure of crystalline materials. In principle, a lattice image is a map of the sample (Coulomb) potential, projected along a zone axis (see, e.g., [1,2]). In practice, it is difficult to extract quantitative information from lattice images. This stems from two primary reasons. First, electrons are multiply scattered during their passage through crystalline samples of realistic thickness ( $\geq 10$  Å). This results in a complex, highly nonlinear relationship between the sample potential and the characteristics of the lattice image. This relationship changes rapidly with the sample thickness, and thus from point to point over the sample. Second, electromagnetic lenses have severe aberrations. The image details thus depend sensitively on the (contrast) transfer function of the microscope, and hence the lens defocus. It is not possible to establish a general relationship between the sample potential and the image features. This has led to the development of "image matching" procedures, whereby the sample structure is inferred by visually comparing simulated images of model structures with experimental results. Extraction of information by this procedure, even at the qualitative level, requires accurate knowledge of the imaging conditions (sample thickness, lens defocus, etc.) [3,4]. These are difficult to measure, and are often poorly known.

Here, we describe an approach, named QUANTITEM, which *measures* the variation of the sample potential from general lattice images of structurally perfect crystalline materials, requiring no knowledge of the imaging conditions [5]. In samples of uniform composition, QUANTITEM can be used to map the topography of buried interfaces in plan view, with near-atomic resolution and sensitivity. Here, we demonstrate this capability for the Si/SiO<sub>2</sub> interface. We show that QUANTITEM topographic images of such *interfaces* are comparable with those obtained from *surfaces* by the scanning tunneling microscope. In samples with compositional nonuniformities, QUANTITEM may be used to map the compositional variation. We demonstrate this by presenting composition maps across Si/GeSi/Si quantum wells. Unlike chemical mapping, QUANTITEM does not rely on

the presence of chemical reflections [6,7], and is thus applicable to general crystalline materials.

To describe the principle of this approach, it is convenient to represent the information content of an image unit cell in vector notation [8]. All the available information in a lattice image is contained in the image intensity distribution. The periodicity of the lattice can be used to divide the image into unit cells, within each of which the intensity distribution is digitized, say  $n \times m$  times. We represent these  $n \times m$  numbers as the components of a (multidimensional) vector, whose position and length describe all the available information. (For a discussion of image localization, see [1,9,10].)

To measure the variation of the projected potential from a lattice image, one must discover how the image changes with the projected potential, under the particular conditions used to obtain the lattice image under analysis. In vector notation, this requires two steps. First, one needs to determine the path traced by the unit cell image vector as the sample potential varies (Fig. 1). This path changes with imaging conditions, and must be determined afresh for each lattice image. Second, one must determine the rate at which this path is traversed as the sample potential changes. This rate need not be a linear

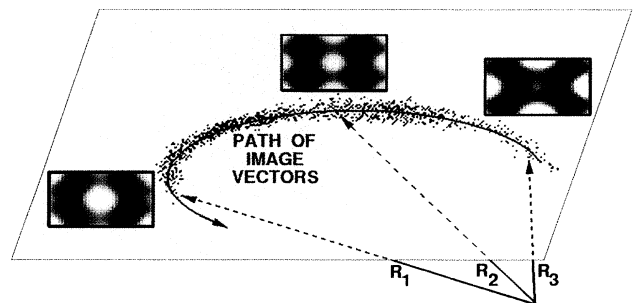


FIG. 1. Lattice image unit cells, and their vector representation  $\mathbf{R}^i$ , for three different sample thicknesses. The cloud of points represents tips of vectors drawn from an experimental image of a (wedge-shaped) Si sample. The path described by the image vectors quantifies the way changes in the sample projected potential affect the lattice image.

function of the potential change. Determination of the path and the rate at which it is traversed quantify the way that changes in the sample potential affect the image.

The path of the image vector can be directly determined from the experimental image by plotting the tips of the image unit cell vectors over the region of interest (Fig. 1). Since all TEM samples are wedge shaped, this directly reveals the path described by the image unit cell vector as the projected potential changes. The rate at which this path is traversed can be measured in one of two ways. In the first, one assumes that no particular thickness is favored over the field of view [11]. The density of points (vector tips) along the path is then inversely proportional to the local rate of path traversal. The total length of the path can be calibrated in terms of sample thickness, by recognizing that lattice images vary periodically with the pendellösung oscillations. This calibrates one period of the path in terms of a known change in thickness, namely, the extinction distance [12].

The second approach to measuring the local rate of path traversal requires high signal-to-noise ratios. In the absence of noise, the atomic nature of the sample gives rise to discrete clusters of points along the path, each representing columns with a given number of atoms. Noise tends to smear these clusters into a continuous distribution. Nevertheless, the signal-to-noise ratio is sometimes adequate to reveal the presence of such clustering of points in Fourier transforms of their density, or by autocorrelation techniques. This allows an absolute determination and calibration of the rate at which the path is traversed as a function of projected potential.

The above discussion notwithstanding, we show below that appropriate parametrization of the path can result in a highly linear relationship between the projected potential and the chosen parameter, obviating the need for local calibration of the rate of path traversal.

We now describe how QUANTITEM may be implemented in practice. The procedure is facilitated by an appropriate choice of reference frame in vector space. We derive a reference frame from the experimental image itself, by extracting a number of "template" vectors from the image. A general unit cell is then expressed in terms of its projections on planes defined by these template vectors. In general, three template vectors suffice, and their choice is not critical [13]. The primary requirement is that the choice of template vectors  $\mathbf{R}^T$  should provide an adequate description of the significant images present. This is easily achieved by extracting a template from each area of the image with distinctly different characteristics.

Analysis of simulated images shows that, in general, the path described by the image vector for potential changes of about half an extinction distance can be well approximated by an ellipse [14]. Figure 1 shows the tips of experimental image unit cell vectors projected onto the plane defined by the three template vectors  $\mathbf{R}_i^T$ . We de-

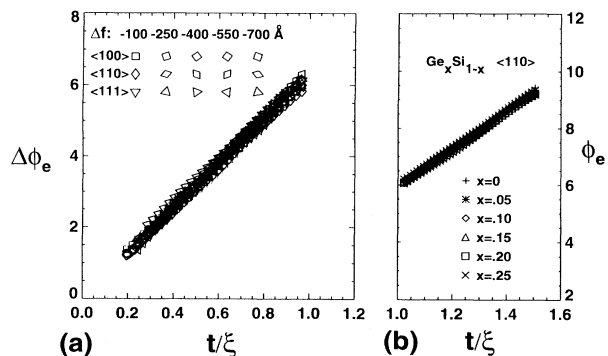


FIG. 2. Variation of ellipse phase angle  $\phi_e$  vs sample thickness  $t$ , normalized to the extinction distance  $\xi$ , simulated for Si (a) and  $\text{Ge}_x\text{Si}_{1-x}$  (b). Note the strong overlap of the points, indicating a universal relation between the variation in  $\phi_e$  and the projected potential for these systems, irrespective of sample thickness, projection direction, and lens defocus.

scribe the path by fitting an ellipse to the experimental points, and parametrize it in terms of the ellipse phase angle  $\phi_e$ . [In two dimensions, a point  $(x, y)$  on an ellipse is given by  $x = a \cos \phi_e$ ,  $y = b \sin \phi_e$ .] For the samples we have investigated, this parametrization yields a universal and linear dependence on the sample potential, irrespective of the imaging conditions. Figure 2 is a plot of the variation of the ellipse angle  $\phi_e$  vs the projected potential for Si in the  $\langle 100 \rangle$ ,  $\langle 111 \rangle$ , and  $\langle 110 \rangle$  projections, and  $\text{Ge}_x\text{Si}_{1-x}$ , over the defocus range  $-100$ – $-700$  Å, and thickness range  $80$ – $420$  Å. These plots were obtained by analyzing simulated images of Si and  $\text{Ge}_x\text{Si}_{1-x}$  in the  $\langle 110 \rangle$  projection. When present, such a universal relationship obviates the need for fresh measurement and calibration of the rate of path traversal in each lattice image.

By presenting experimental images of the atomic roughness at Si/SiO<sub>2</sub> interfaces in plan view, we show that QUANTITEM may be used to reveal the topography of buried interfaces with high spatial resolution and sensitivity. Figure 3(a) is a  $\langle 100 \rangle$  lattice image of a Si sample, after a final rinse in an anisotropic etch (KOH in H<sub>2</sub>O) and the formation of a native oxide ( $\sim 15$  Å thick on each surface). Figure 3(b) is a QUANTITEM map of the thickness variations in (the crystalline part of) the SiO<sub>2</sub>/Si/SiO<sub>2</sub> sample, with height representing thickness.

TABLE I. Thickness and chemical sensitivity of QUANTITEM. Best values were obtained by median filtering over  $2 \times 2$  image unit cells.

System	Cell size (Å <sup>2</sup> )	Sensitivity	
		Typical	Best
Si $\langle 100 \rangle$	$2.7 \times 2.7$	15.1 Å	3.2 Å
Si $\langle 110 \rangle$	$3.8 \times 5.4$	5.3 Å	2.0 Å
Si $\langle 111 \rangle$	$2.2 \times 3.8$	11.0 Å	3.2 Å
$\text{Ge}_{0.25}\text{Si}_{0.75} \langle 110 \rangle$	$3.8 \times 5.4$	5.4 at. % Ge	2.4 at. % Ge

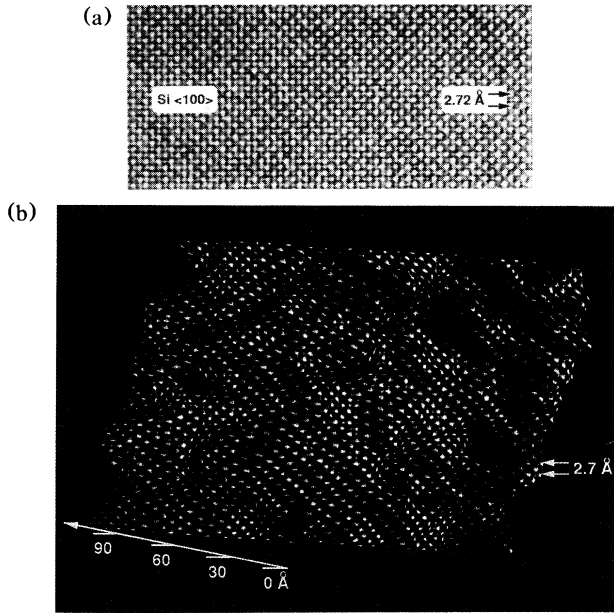


FIG. 3. (a) Lattice image of SiO<sub>2</sub>/Si/SiO<sub>2</sub> sample, viewed in  $\langle 100 \rangle$  plan view. The sample was formed by anisotropic etching of Si in KOH, followed by formation of a native oxide. Two Si/SiO<sub>2</sub> interfaces are seen superimposed. (b) QUANTITEM map of the thickness of crystalline Si sandwiched between the two SiO<sub>2</sub> layers. Height represents sample thickness. This topographic map, deduced from (a) above, directly reveals the superimposed roughness of the two Si/SiO<sub>2</sub> interfaces. Note the pyramidal hillocks produced by the anisotropic etch.

Since the sample contains two Si/SiO<sub>2</sub> interfaces, the variations reveal the superimposed roughness of the two Si/SiO<sub>2</sub> interfaces in plan view. The formation of pyramidal hillocks due to the anisotropic nature of the etch is clear. Such structures are absent when the Si surface is etched isotropically. Quantitative error analysis yields the sensitivity estimates shown in Table I. It is clear that two monolayer thickness variations can be readily measured, and in favorable circumstances, monolayer thickness sensitivity may be obtained by spatial (median) averaging over four image unit cells. Figure 3(b) constitutes the first quantitative, high resolution, topographic image of a buried interface in plan view.

We now describe how QUANTITEM may be used to measure the chemical transition between two regions of known composition in crystalline materials. In the absence of chemical reflections [7], a lattice image essentially measures the sample projected potential. Changes in sample thickness and composition must therefore be considered on the same footing. This is demonstrated by Fig. 2, in which the ellipse phase angle  $\phi_e$  shows the same dependence on sample thickness for Si and Ge<sub>0.25</sub>Si<sub>0.75</sub>, provided the thicknesses are normalized to the extinction distance for each material.

Changes in composition have two consequences. First, the path described by the vector can be changed. When

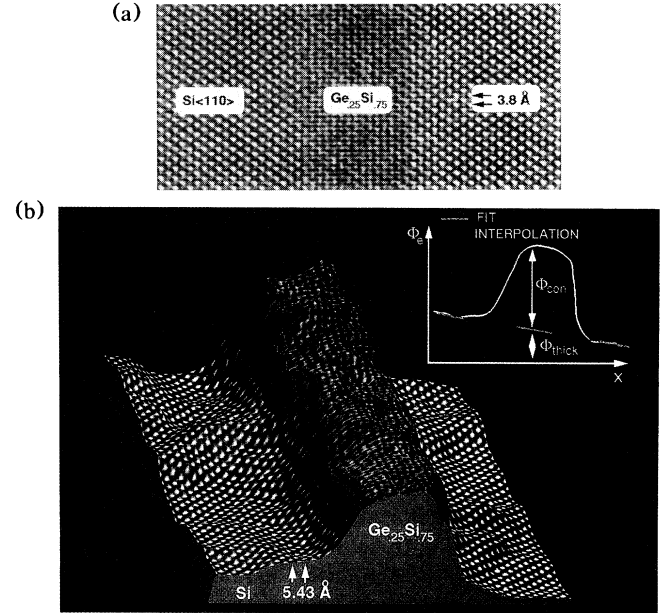


FIG. 4. (a) Lattice image of Si/Ge<sub>0.25</sub>Si<sub>0.75</sub>/Si quantum well structure, viewed in  $\langle 110 \rangle$  cross section. (b) Map of ellipse phase angle  $\phi_e$  across the image shown in (a) above. Note the variations in the Si region, indicating significant thickness changes. Inset: schematic representation of the effect of composition on  $\phi_e$ . The heavier GeSi causes  $\phi_e$  to advance more rapidly. The variation of thickness across the field of view means that part of the change in  $\phi_e$  is due to composition, part due to thickness change.

present, this can be readily discerned by plotting the experimental vectors in regions of known composition. Second, the extinction distance is altered, which changes the rate at which the path is traversed in each material. Heavier materials advance the phase more rapidly (Fig. 4). QUANTITEM exploits this latter effect to determine the composition of an image unit cell. Consider a target

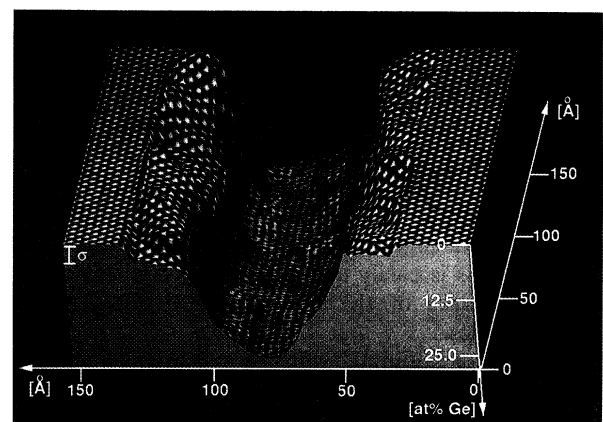


FIG. 5. QUANTITEM composition map deduced from Fig. 4. Height represents Ge concentration, the bar one-sigma accuracy.

unit cell of unknown thickness and composition, and assume for the moment that its thickness is known. In outline, QUANTITEM proceeds as follows [(Fig. 4(b), inset): (i) It measures the amount by which the ellipse phase angle  $\phi_e$  of the target unit cell is advanced from a reference unit cell in a region of known composition; (ii) it subtracts off the part due to the thickness change; (iii) it ascribes the remainder to changes in the extinction distance, and hence composition. Since the extinction distance can be easily calculated and/or measured, this directly yields the composition of the target unit cell.

To determine the sample thickness at the target unit cell, we map the sample thickness over regions of known composition, and fit a two-dimensional model function (surface) to the data, so as to obtain an accurate description of the undulations in the sample thickness. We then infer the sample thickness at the target unit cell by interpolating the model function between the adjoining regions of known composition [Fig. 4(b), inset]. Quantitative procedures are used to determine the uncertainty with which the thickness at the target cell has been inferred.

Figure 4(a) is a  $\langle 110 \rangle$  cross-sectional lattice image of a Si/Ge<sub>0.25</sub>Si<sub>0.75</sub>/Si quantum well [15]. Figure 4(b) shows the variation of the ellipse phase angle  $\phi_e$  across the image, as determined by QUANTITEM. The variation of  $\phi_e$  over the regions away from the interfaces clearly reveals significant thickness changes, both locally and across the  $\sim 150$  Å square field of view. These variations can be reproduced by a model function with a (one-sigma) accuracy of  $\sim 3.5$  Å. As shown in the inset of Fig. 4(b), in regions of unknown composition, the sample thickness is inferred by interpolation. Once the sample thickness at a target cell is determined, its composition is deduced from the part of  $\Delta\phi_e$  not due to thickness change.

Figure 5 is a QUANTITEM composition map across a Si/Ge<sub>0.25</sub>Si<sub>0.75</sub>/Si quantum well. The height represents the Ge concentration. This image represents the first quantitative microscopic map of the compositional change across the important Si/Ge<sub>x</sub>Si<sub>1-x</sub> interface, directly revealing its roughness at high resolution. (See Table I.)

The implementation of QUANTITEM requires attention to important practical factors, such as the nonlinearities and geometrical distortions introduced by the recording medium, and the tradeoff between noise and spatial resolution. We have established that such factors do not affect the practical implementation of QUANTITEM, or have developed procedures to measure and/or reduce their consequences [13].

We now discuss the more general implications of our work. There can be no single route to quantitative electron microscopy. However, we have described a means for direct measurement of the sample projected potential from general lattice images. This approach is based on the notion that imaging conditions do not need to be individually known, or controlled. Their combined effect sim-

ply produces a relationship between the projected potential and the image features, which can be extracted directly from each experimental image. Here we have demonstrated the ability of QUANTITEM to yield high resolution topographic maps of *buried* interfaces in plan view. This opens the way for the study of a variety of important interfacial reactions at the atomic level, such as surface roughening during oxidation. The ability to map compositional variations in general systems is a significant step toward investigating the relaxation of general multilayered systems and their point defect reactions [7]. More generally, QUANTITEM constitutes a rapid and robust means of extracting quantitative information from lattice images.

We acknowledge valuable discussions with G. Higashi and Y. LeCun, and expert technical assistance from J. A. Rentschler. The GeSi/Si samples were kindly provided by J. C. Bean and J. Bevk.

- [1] J. C. H. Spence, *Experimental High Resolution Electron Microscopy* (Clarendon, Oxford, 1981).
- [2] K. H. Downing, H. Meisheng, H-R. Wenk, and M. A. O'Keefe, *Nature (London)* **348**, 525 (1990).
- [3] A. Bourret, J. L. Rouviere, and J. M. Penisson, *Acta Crystallogr. Sect. A* **44**, 838 (1988).
- [4] M. A. O'Keefe, U. Dahmen, and C. J. D. Hetherington, *Mater. Res. Soc. Symp. Proc.* **159**, 453 (1990).
- [5] For the systems considered here, a unique relationship between the projected potential and the image can be established. A detailed discussion will be presented elsewhere.
- [6] A. Ourmazd, D. W. Taylor, J. Cunningham, and C. W. Tu, *Phys. Rev. Lett.* **62**, 933 (1989).
- [7] A. Ourmazd, *Mater. Sci. Rep.* **9**, 201 (1993).
- [8] A. Ourmazd, D. W. Taylor, M. Bode, and Y. Kim, *Science* **246**, 1571 (1989).
- [9] We have previously shown that under appropriate imaging conditions, the information content of an image unit cell is directly related to the projected potential of a region of the same cross section in the sample. See F. H. Baumann, M. Bode, Y. Kim, and A. Ourmazd, *Ultramicroscopy* **47**, 167 (1992).
- [10] L. D. Marks, *Ultramicroscopy* **18**, 33 (1985).
- [11] This is not as restrictive as assuming a "linear" wedge with a constant slope. However, it does require that, on average, the sample not systematically deviate from a linear wedge.
- [12] In cases where the pendellösung oscillations cannot be characterized by a single extinction distance, a "local" extinction distance can be used to describe these oscillations.
- [13] For a discussion see C. Kisielowski, P. Schwander, F. H. Baumann, Y. Kim, and A. Ourmazd (to be published).
- [14] For larger thickness changes, the variation of defocus due to the wedge shape of the sample can cause significant departures in the path from an ellipse. While convenient, it is not necessary that the path should be an ellipse. Any path can be parametrized, and the parameter related to the projected potential as described above.
- [15] All images presented here were obtained with a JEOL 4000EX TEM, operating at 400 kV.

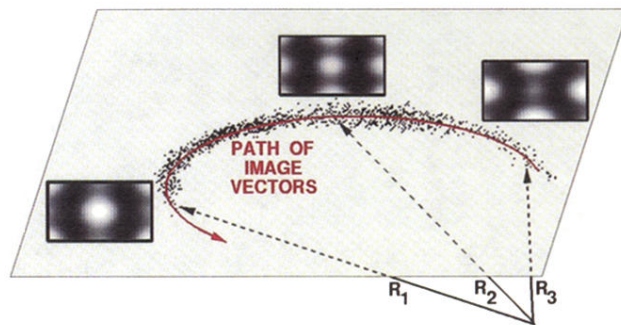


FIG. 1. Lattice image unit cells, and their vector representation  $R^i$ , for three different sample thicknesses. The cloud of points represents tips of vectors drawn from an experimental image of a (wedge-shaped) Si sample. The path described by the image vectors quantifies the way changes in the sample projected potential affect the lattice image.

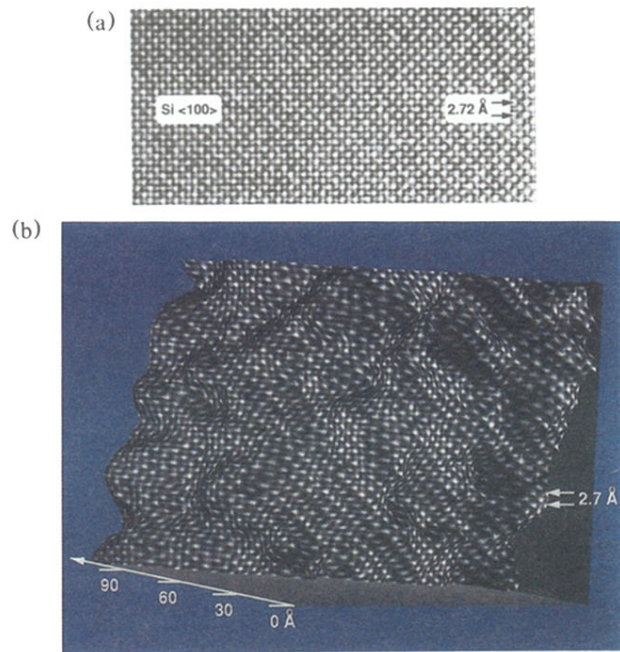


FIG. 3. (a) Lattice image of  $\text{SiO}_2/\text{Si}/\text{SiO}_2$  sample, viewed in  $\langle 100 \rangle$  plan view. The sample was formed by anisotropic etching of Si in KOH, followed by formation of a native oxide. Two Si/SiO<sub>2</sub> interfaces are seen superimposed. (b) QUANTITEM map of the thickness of crystalline Si sandwiched between the two SiO<sub>2</sub> layers. Height represents sample thickness. This topographic map, deduced from (a) above, directly reveals the superimposed roughness of the two Si/SiO<sub>2</sub> interfaces. Note the pyramidal hillocks produced by the anisotropic etch.

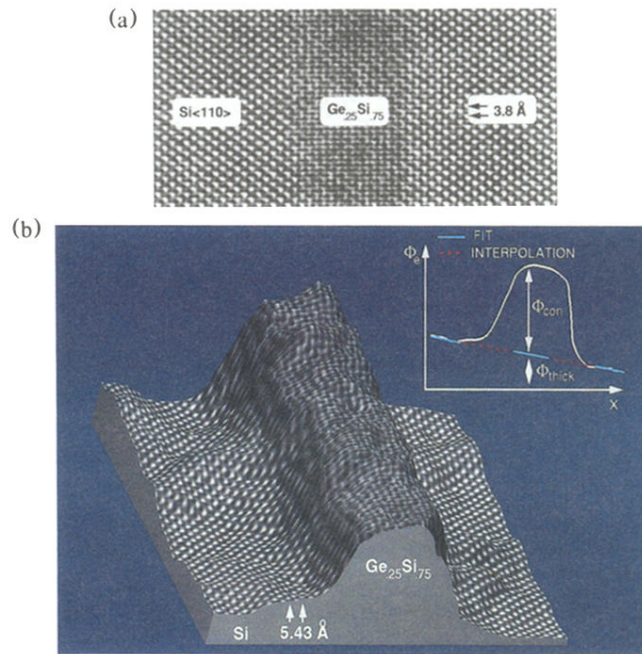


FIG. 4. (a) Lattice image of Si/Ge<sub>0.25</sub>Si<sub>0.75</sub>/Si quantum well structure, viewed in <110> cross section. (b) Map of ellipse phase angle  $\phi_e$  across the image shown in (a) above. Note the variations in the Si region, indicating significant thickness changes. Inset: schematic representation of the effect of composition on  $\phi_e$ . The heavier GeSi causes  $\phi_e$  to advance more rapidly. The variation of thickness across the field of view means that part of the change in  $\phi_e$  is due to composition, part due to thickness change.

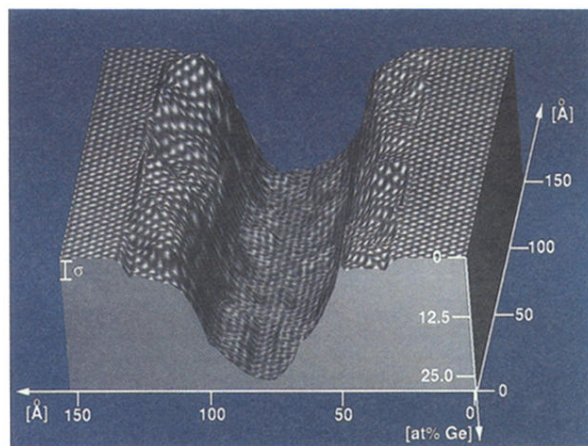


FIG. 5. QUANTITEM composition map deduced from Fig. 4. Height represents Ge concentration, the bar one-sigma accuracy.